Novel compound heterozygous mutations for lipoprotein lipase deficiency: a G-to-T transversion at the first position of exon 5 causing G154V missense mutation and a 5′ splice site mutation of intron 8

Yasuyuki Ikeda,[1,*] Atsuko Takagi,[†] Yuusei Nakata,[§] Yasuhiko Sera,[§] Sumio Hyoudou,[§] Kazuko Hamamoto,[§] Yoshikazu Nishi,[§] and Akira Yamamoto[**]

Departments of Etiology and Pathophysiology* and Pharmacology,[†] National Cardiovascular Center Research Institute, 5-7-1 Fujishirodai, Suita, Osaka 565-8565, Japan; Department of Pediatrics,[§] Hiroshima Red Cross Hospital, Hiroshima 730-8619, Japan; and Fourth Department of Internal Medicine,[**] Hyogo College of Medicine, Hyogo 663-8131, Japan

Abstract **We systematically investigated the molecular defects causing a primary LPL deficiency in a Japanese male infant (patient DI) with fasting hyperchylomicronemia (type I hyperlipoproteinemia) and in his parents. Patient DI had neither LPL activity nor immunoreactive LPL mass in the pre- and post-heparin plasma. The patient was a compound heterozygote for novel mutations consisting of a G-to-T transversion at the first nucleotide of exon 5 [+1 position of 3′ acceptor splice site (3′-ass) of intron 4] and a T-to-C transition in the invariant GT at position +2 of the 5′ donor splice site (5′-dss) of intron 8 (Int8/5′-dss/t(+2)c). The G-to-T transversion, although affecting the 11 nucleotide of the 3′-consensus acceptor splice site, resulted in a substitution of Gly[154] to Val (G154V; GG[716]C→GTC). The mutant G154V LPL expressed in COS-1 cells was catalytically inactive and hardly released from the cells by heparin. The Int8/5′-dss/t(+2)c mutation inactivated the authentic 5′ splice site of intron 8 and led to the utilization of a cryptic 5′-dss in exon 8 as an alternative splice site 133 basepairs upstream from the authentic splice site, thereby causing joining of a part of exon 8 to exon 9 with skipping of a 134-bp fragment of exon 8 and intron 8. These additional mutations in the consensus sequences of the 3′ and 5′ splice sites might be useful for better understanding the factors that are involved in splice site selection in vivo.**—Ikeda, Y., A. Takagi, Y. Nakata, Y. Sera, S. Hyoudou, K. Hamamoto, Y. Nishi, and A. Yamamoto. **Novel compound heterozygous mutations for lipoprotein lipase deficiency: a G-to-T transversion at the first position of exon 5 causing G154V missense mutation and a 5′ splice site mutation of intron 8.** ***J. Lipid Res.*** **2001.** 42: **1072–1081.**

Supplementary key words LPL gene mutation • hypertriglyceridemia • first nucleotide • first base • acceptor splice site • donor splice site • cryptic splice site

Type I hyperlipoproteinemia (hyperchylomicronemia) has been reported to be caused mainly by a deficiency of LPL (EC 3.1.1.34), which is responsible for hydrolyzing the triglycerides in chylomicrons and VLDL (1, 2). Human LPL is a glycoprotein enzyme with a molecular mass of 61 kDa (3). LPL cDNA predicts a translated molecular mass of 50,394 with 448 amino acid residues in the absence of any sugar moiety (4). The human LPL gene, 30 kb in length, is located on chromosome 8p22 (5), and consists of 10 exons (6–8): exons 1 through 9 contain coding regions, whereas exon 10 contains a 3′ noncoding region. LPL is mainly synthesized in adipocytes and is anchored on the cell surface by a proteoglycan chain (9, 10), where LPL interacts with chylomicrons and VLDL in the circulation.

Intravenous injection of heparin releases significant amounts of both catalytically active LPL and hepatic triglyceride lipase (HTGL) into the circulation (11, 12), whereas small amounts of both lipases are detected as catalytically inactive forms in the plasma (pre-heparin plasma) (12). HTGL is thought to play a role in further hydrolysis of the triglycerides remaining in chylomicrons and VLDL catabolized by LPL (13). Plasma obtained after injection of heparin (post-heparin plasma, PHP) is usually used as a clinical sample for detecting abnormalities of LPL and HTGL. LPL gene analysis has been performed on subjects with an LPL abnormality, and homozygous or compound heterozygous mutations in the LPL gene have been identified in subjects with type I hyperlipoproteinemia. To date, over 60 distinct mutations in the LPL gene have been re-

Abbreviations: 5′-dss, 5′ donor splice site; 3′-ass, 3′ acceptor splice site; DI, patient's initials; EIA, enzyme immunoassay; FECH, ferrochelatase; HEXA, β-hexosaminidase A; HTGL, hepatic triglyceride lipase; PHP, post-heparin plasma; precursor mRNA, pre-mRNA; RHAG, RH antigen; SIIA, selective immunoinactivation assay; SSCP, single-strand conformation polymorphism; TBE, Tris-boric acid-EDTA.

[1] To whom correspondence should be addressed.
e-mail: yikeda@ri.ncvc.go.jp

ported in various ethnic groups, including the Japanese (2). Most of the mutations are missense and nonsense mutations, and found in exons 4, 5, and 6 of the LPL gene (2), which constitute a large amino N-terminal domain containing the catalytic function (14).

Splice site (exon/intron boundary) mutations are a relatively common cause of human genetic disease. Generally, splicing of precursor (pre)-mRNA requires a consensus sequence at the boundaries of the exons and introns: the sequence of $(A_{32}/C_{37})A_{58}G_{78}/g_{100}$ t_{100} a_{57} a_{71} g_{84} t_{47} presents at the 5′ donor splice site (5′-dss) and the sequence of y_{76} y_{78} y_{82} y_{86} y_{82} y_{79} y_{85} y_{83} y_{87} y_{86} n c_{74} a_{100} g_{100}/G_{49} at the 3′ acceptor splice site (3′-ass; y = pyrimidine, t or c; n = any base; subscript numerals refer to percentage frequency of occurrence) (15, 16). In particular, the invariant "gt" and "ag" motifs of introns are essential for normal splicing. A few cases of invariant dinucleotide mutations in the LPL gene have been reported, and all cases indeed result in aberrant splicing (17–19). For 5′-dss and 3′-ass, the correlation between splicing and naturally occurring mutations in the vicinity of the invariant "gt" or "ag" has also been examined and summarized (19). Little information is available regarding mutation of the first nucleotide G in exon at 3′-ass relating to aberrant splicing (20–22), and no reports are available for the LPL gene.

In the present article, we describe in detail a molecular defect of LPL of fasting hyperchylomicronemia due to primary LPL deficiency detected in a Japanese male infant (patient DI) and in his parents. Patient DI was a compound heterozygote for novel mutations consisting of a G-to-T transversion at the first nucleotide of exon 5 (+1 position at the 3′-ass of intron 4) and a T-to-C transition in the invariant "gt" at position +2 of the 5′-dss of intron 8 (Int8/5′-dss/t(+2)c). The G-to-T transversion (G/GC→G/TC) within a consensus sequence at the first position of exon 5 might have a possibility to cause aberrant splicing of LPL pre-mRNA, but it led to a substitution of Gly^{154} to Val (G154V), which resulted in a catalytically inactive LPL. Also, molecular characterization of aberrantly spliced LPL mRNA, induced by the Int8/5′-dss/t(+2)c allele, and the utilization of a cryptic splice site in exon 8 due to this mutation are described.

MATERIALS AND METHODS

Patient and his parents

Patient DI, a 2-month-old Japanese male, was referred from Hiroshima Red Cross Hospital to our Institute (National Cardiovascular Center Research Institute) for examination of the etiology underlying his severe hypertriglyceridemia. There was no family history of consanguinity in patient DI's kindred. His father and mother were also investigated. As a control group for the patient, four healthy male subjects (age 2.1 ± 0.9 years; mean ± SD) were recruited with their parents' agreement. Also, adult healthy volunteers (n = 100; 56 males and 44 females) between the ages of 23 and 69 years were studied as a control group. Genetic analysis of patient DI and his parents was performed after obtaining their informed consent, which was approved by the Institutional Ethics Committee.

Laboratory and biochemical tests

Serum sample was prepared from blood obtained after the subjects had fasted overnight. Serum lipoproteins were fractionated into five classes according to their density by sequential flotation ultracentrifugation (23): chylomicron (d < 1.006 g/ml), VLDL (d < 1.006 g/ml), intermediate density lipoprotein (d = 1.006–1.019 g/ml), LDL (d = 1.019–1.063 g/ml), and HDL (d = 1.063–1.21 g/ml). The triglyceride and cholesterol concentrations in the serum and the fractionated lipoproteins were measured by enzymatic methods according to the manufacturer's instructions (Triglyceride G-Test and Cholesterol C-Test kits; Wako Chemical Co., Kyoto, Japan).

Measurement of LPL and HTGL activities and immunoreactive masses in plasma

The subjects were fasted overnight, and blood samples were collected in tubes containing 2Na-EDTA (1 mg/ml) before and 10 min after the injection of heparin (30 U/kg of body weight). LPL and HTGL activities in PHP were measured with gum arabic-emulsified tri(9,10-^{3}H)olein (specific activity: 330.4 GBq/mole) as the substrate by selective immunoinactivation assay (SIIA), as reported previously (3, 12). Both enzyme activities were expressed as micromoles of free fatty acid released per hour per milliliter of enzyme solution, unless stated otherwise.

A one-step sandwich-enzyme immunoassay (EIA) for LPL mass quantification was performed using a Markit-F LPL kit (Dainippon Pharmaceutical, Osaka, Japan) and sandwich-EIA for HTGL mass quantification was also carried out, as described previously (12). The immunoreactive LPL and HTGL masses in pre-heparin plasma and in PHP were measured, and the increments in the LPL and HTGL masses were calculated as the difference between the masses in pre-heparin plasma and PHP, respectively. The enzyme mass values of the increments were expressed as nanograms of LPL and HTGL per milliliter of plasma, respectively.

Genomic DNA extraction and Southern blot analysis

Genomic DNA was isolated from the peripheral whole blood of patient DI, his parents, and normal controls. Southern blot analysis was performed after digestion of the DNA with the appropriate restriction enzymes (*Hind*III and *Pvu*II) using ^{32}P-labeled HLC601 (24) as a probe according to the standard procedure (25).

Fluorescence-based SSCP analysis

The individual exons and their flanking regions (1DU, 1DD through 9) in the LPL gene were each amplified enzymatically from the genomic DNA by the PCR method using a pair (F and R) of fluorescent substance (Cy5)-labeled primers, in which the Cy5 was attached to the 5′ end of individual 5′ flanking and intron sequences of the LPL gene, as described previously (26). Fluorescence-based SSCP analysis was performed by electrophoresis using a 6% polyacrylamide gel containing 10% glycerol and Tris-boric acid-EDTA (TBE) buffer, pH 7.7, at temperatures of 15°C, 20°C, 25°C, and 30°C. The SSCP pattern was analyzed with an ALFexpress DNA sequencer equipped with AlleleLinks™ software (Pharmacia Biotech, Uppsala, Sweden) according to the manufacturer's directions.

Direct DNA sequencing

Templates (1DU, 1DD through 9) for DNA sequencing were enzymatically amplified from the genomic DNA of the subjects by PCR using each pair (F and R) of primers tagged with 5′-TGTAAAACGACGGCCAGT-3′ (forward) and 5′-CAG GAAAACGACGGCCAGT-3′ (reverse), as previously reported (26). The sense strand of the amplified template DNA was directly se-

quenced with a Seq-F primer of 5′-Cy5-labeled TGTAAAAC GACGGCCAGT-3′, and the antisense strand of the template DNA with a Seq-R primer of 5′-Cy5-labeled CAGGAAAACGACG GCCAGT-3′ using Thermo Sequenase Fluorescent-labeled primer cycle sequencing kit with 7-deaza-dGTP (Amersham Life Science, Tokyo, Japan). The reaction mixture was mixed with the stop/loading dye and electrophoresed on a 6% polyacrylamide and 7 M urea gel. The DNA sequence pattern was determined with an ALFexpress DNA sequencer equipped with ALFwin™ software (Pharmacia Biotech), according to the manufacturer's directions. Both the nucleotide sequence and amino acid positions of the LPL gene mutations detected here correspond to the human LPL cDNA sequence (4).

Mutagenic PCR for detection of the mutant allele causing splicing mutation in intron 8 of the LPL gene

LPL gene-exon 8 and its boundaries were amplified by PCR using the Exon-8F primer and the Exon-8R primer (No. 341) containing a single base mismatch of a T-to-C transition (5′-CTAAAGTGAAGGAAGAAAAATACATTCAAT-3′; the mismatched nucleotide is indicated by the underline). Mutagenic PCR introduced a *Mfe*I restriction enzyme site in intron 8 of the LPL gene of patient DI's DNA, where this site was absent in normal individuals. The amplified DNA (271-bp fragment) was digested with 10 units of *Mfe*I restriction enzyme (New England BioLabs; Beverly, MA) overnight at 37°C. The resulting DNA fragments were analyzed on a 4% NuSieve agarose gel (FMC BioProducts, Rockland, ME). DNA bands were visualized by staining with ethidium bromide.

RT-PCR amplification of LPL cDNA, its size determination, and sequencing

Monocyte-derived macrophages were prepared by culturing monocytes isolated from 50 ml of peripheral blood from patient DI's father, mother, and normal subjects by the Ficoll-Hypaque gradient method as described previously (27). Poly $(A)^+$ RNA was isolated from monocyte-derived macrophages using a QuickPrep® Micro mRNA Purification kit (Amersham Pharmacia Biotech, Tokyo, Japan). The isolated mRNA (57 ng) was reverse-transcribed in a 33-μl reaction mixture containing 100 pmol of random hexamers using a kit of Ready-To-Go You-Prime First-Strand Beads (Amersham Pharmacia Biotech). The reverse-transcribed cDNA was used as a template for amplification of LPL cDNA by PCR with two-step reactions. First, LPL cDNA of the patient's mother was amplified by PCR using a primer (No. 26, 5′-ACACCAAACTGGTGGGACAG-3′) and LPL cDNA of the patient's father was amplified by PCR using a primer (No. 354, 5′-TCTTCCATTACCAAGTAAAGATT-3′). Subsequently, LPL cDNA was further amplified from the first PCR-amplified cDNA using a pair of forward (No. 355, 5′-TGGCCCGGTTTATCAACTG GATG-3′) and reverse (No. 28, 5′-ATGAAGAGATGAATGGAGCG-3′) nested primers for the patient's mother, and a pair of forward (No. 352, 5′-TGGCCGAGAGTGAGAACATC-3′) and reverse (No. 353, 5′-GACACTTTCTCCCTAGAACAG-3′) nested primers for the patient's father. The size of the amplified LPL cDNA fragments was determined by 4% NuSieve agarose gel electrophoresis. The LPL cDNA bands were extracted from the agarose gel and cloned into a vector of pCRII (Invitrogen®, San Diego, CA). The cloned LPL cDNA was sequenced using the fluorescent Seq-F and Seq-R sequencing primers as described above.

Construction of mutant LPL cDNA by site-directed mutagenesis

Normal human LPL cDNA (HLC601), subcloned into the phagemid Bluescript SK II M13 (−) vector, was used as a template for site-specific mutagenesis. Mutant G154V LPL cDNA was generated with the mutagenic oligonucleotide primer (No. 272) of 5′-AAGGAAGCCTTGGAGAAAGGGCTC-3′ using a Mutan®-K kit (Takara, Kyoto, Japan). The underlined base of the primer is the specifically mutated base. The normal LPL cDNA or G154V LPL cDNA fragment was subcloned into an expression vector (pRc/CMV; Invitrogen®, San Diego, CA) with the cytomegalovirus early promoter.

Expression of normal LPL cDNA and mutant LPL cDNA in COS-1 cells, LPL enzyme assay, and Northern blot analysis

Normal LPL cDNA, G154V LPL cDNA-pRc/CMV, or a pRc/CMV expression vector, was transfected into COS-1 cells by an electroporation method using a Bio-Rad Gene Pluser II according to the manufacturer's instructions. A β-galactosidase expression plasmid (pCH110; Pharmacia Biotech) was co-transfected into the above expression system as an internal standard in order to assess the efficiency of expression. The transfected COS-1 cells were plated into 10-cm dishes containing 10 ml of DMEM supplemented with 10% heat-inactivated fetal calf serum, and cultured. After 2.5 days of culture, the medium was removed, and the cells were washed with phosphate-buffered saline. The washed cells were treated three times for 5 min at room temperature with 0.5 ml of DMEM containing 10% fetal calf serum and 10 units of heparin in order to release LPL bound to the cell surface. The pooled medium (a total volume of 1.5 ml) containing heparin-released LPL was immediately frozen in liquid nitrogen and stored at −80°C until used for the assay. The remaining cells in the dish were washed with phosphate-buffered saline, harvested in 2.0 ml of Cell-Solubilizer (20 mM sodium phosphate buffer, pH 7.4, containing 1 mM EDTA, 10% glycerol, 3 mM benzamidine, 3.1 μM aprotinin, heparin (10 U/ml), and 0.15% Briji-35), and solubilized by 1 min of sonication using a Branson sonicator. The cell lysate (2.0 ml) was centrifuged to remove cell debris, flash-frozen, and stored at −80°C. The LPL activity and immunoreactive LPL mass were determined as described above, and these values were corrected based on the β-galactosidase activity co-expressed in COS-1 cells.

Poly$(A)^+$ RNA was prepared from the COS-1 cells transfected with normal LPL cDNA and G154V LPL cDNA-pRc/CMV, or pRc/CMV expression vector, using a QuickPrep® Micro mRNA Purification Kit (Pharmacia Biotech) according to the supplier's directions. Northern blot analysis of the poly$(A)^+$ RNA was performed by using ^{32}P-labeled HLC601 (24) for LPL mRNA and ^{32}P-labeled human glyceraldehyde-3-phosphate dehydrogenase cDNA (Cayman Chemical, Ann Arbor, MI) as a probe, according to the standard procedure (25).

RESULTS

Laboratory data, LPL activity, and immunoreactive LPL mass of patient DI and his parents

Data are shown in **Table 1**. Patient DI exhibited a high plasma triglyceride concentration (1,981 mg/dl) due to massive accumulation of chylomicrons, which was 13.2 times higher than the upper limit (150 mg/dl) of the control. His serum cholesterol (172 mg/dl) was within the control range, whereas LDL and HDL cholesterols were both about one-seventh of the control. Patient DI was diagnosed as having primary type I hyperlipoproteinemia according to the WHO classification of phenotype expression (2). His mother was normolipidemic, whereas his father showed mild hypertriglyceridemia.

TABLE 1. Laboratory data and LPL activity and immunoreactive LPL mass of patient DI and his parents

Data	Subjects			
	Patient DI	Mother	Father	Control (n = 4)
Age	0.5 months	26 years	38 years	2.1 ± 0.9 years
Sex	Male	Female	Male	Male
Serum-TG (mg/dl)	1981	99	273	100 ± 8
(CM+VLDL)-TG (mg/dl)	1899	61	215	38 ± 9
Serum-Chol (mg/dl)	172	182	205	168 ± 13
LDL-Chol (mg/dl)	15	104	111	102 ± 16
HDL-Chol (mg/dl)	7	38	36	47 ± 7
WHO-type	Type I	Normal	Type IV	Normal
LPL activity (μmol/h/ml)	ND	5.6	5.6	9.8 ± 2.5
LPL mass (ng/ml)	ND	122	141	193 ± 42
HTGL activity (μmol/h/ml)	33.2	39.3	28.0	22.5 ± 9.0
HTGL mass (ng/ml)	2,193	3,037	2,115	1,365 ± 568
LPL genotype	G154V/ Int8/5′dss/t(+2)c	Heterozygote of G154V	Heterozygote of Int8/5′dss/t(+2)c	

The control subjects' LPL and HTGL activities and masses were from adult healthy volunteers (n=100). The LPL genotypes are derived from results presented in Figs. 1 and 2. CM, chylomicron; Chol, cholesterol; ND, not detectable.

They exhibited normal levels for plasma cholesterol concentration.

Patient DI exhibited an absence of LPL activity in PHP, and LPL mass value was almost zero (Table 1), resulting in a diagnosis of primary LPL deficiency. The LPL activities and masses of his parents were about 50% of the mean LPL values of normal subjects, suggesting that they are heterozygous for LPL deficiency. The HTGL activities and mass values of all members were above the normal range.

Identification of LPL gene mutation site of patient DI and carrier status of his parents

The gross structure of patient DI's LPL gene was examined by Southern blot analysis, and no appreciable deletion or insertion in the LPL gene was detected (data not shown). Each DNA segment encompassing an exon and its flanking regions, as well as the 5′-upstream region of the LPL gene, were amplified by PCR and analyzed by the SSCP method. Anomalous PCR-SSCP patterns were found for exon 5 and exon 8 and their flanking regions in the patient, indicating that patient DI had heteroallelic mutations in exons 5 and 8, respectively (data not shown). Thus, patient DI was surmised to be a compound heterozygote for mutations in exons 5 and 8 of the LPL gene.

The mutation site in patient DI's LPL gene exon 5 was determined by directly sequencing the DNA segments encompassing exon 5 and its flanking regions. Only one apparent nucleotide substitution was identified, at position 716 of exon 5 (the first nucleotide of exon 5): two distinct peaks were detected at that position, one derived from the variant allele and the other from the normal allele. Nucleotide G^{716}, at the second position of the GGC codon coding for Gly^{154} in the normal allele, was substituted to T in the variant allele, thereby generating a Val codon (GTC) (GG^{716}C→GTC/Gly^{154}→Val; G154V; **Fig. 1**). In patient DI's LPL gene exon 8 and its boundaries, a single T-to-C transition was identified at the +2 position of intron 8 (the second nucleotide of the invariant GT in intron 8): two distinct peaks were detected at that position, one (the nucleotide C) derived from the variant allele and the other (the nucleotide T) from the normal allele (**Fig. 2**). This mutation was designated Int8/5′-dss/t(+2)c. No abnormalities were detected from DNA segments encompassing the other exons and their boundaries.

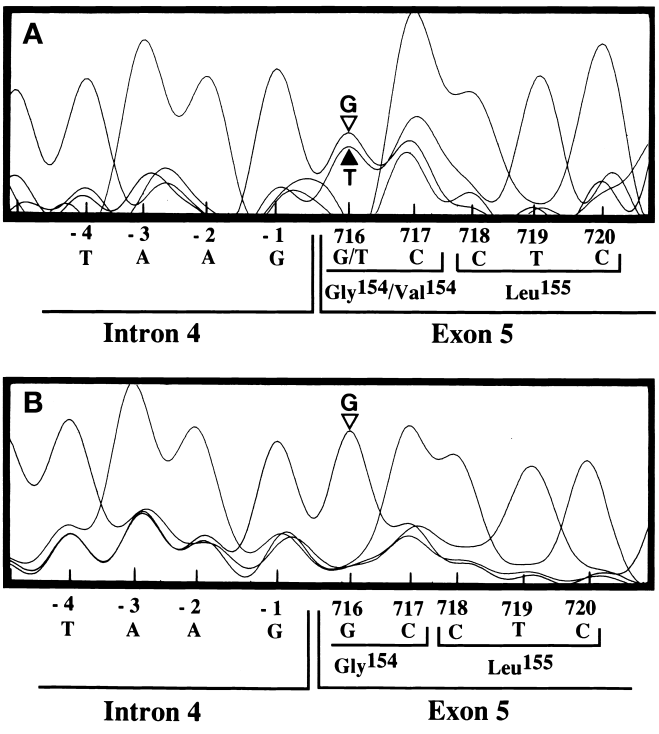

Fig. 1. Identification of the mutation site in exon 5 and its flanking regions of patient DI's LPL gene. Nucleotide sequence patterns of a part of the sense strand from exon 5 and its flanking regions of patient DI (A) and control (B) are shown. A: Two significant peaks were detected at position 716, which is the first position of exon 5: nucleotide G^{716} (indicated by the open triangle) is from the normal allele, whereas nucleotide T^{716} (indicated by the solid triangle) is from the G154V allele. B: One single peak was detected at position 716, representing nucleotide G^{716} (indicated by the open triangle) of the normal allele.

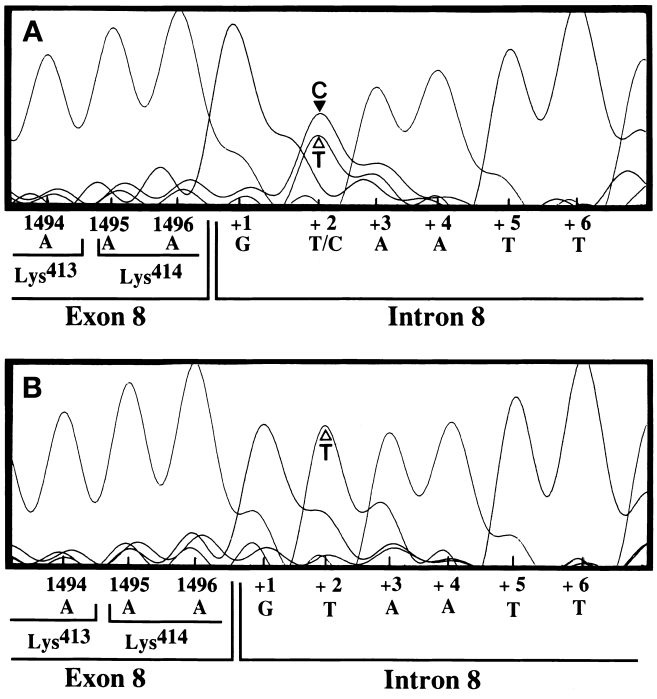

Fig. 2. Identification of the mutation site in exon 8 and its flanking regions of patient DI's LPL gene. Nucleotide sequence patterns of a part of the sense strand from exon 8 and its flanking regions of patient DI (A) and control (B) are shown. A: Two significant peaks were detected at the +2 position of intron 8: nucleotide T (indicated by the open triangle) is from the normal allele, whereas nucleotide C (indicated by the solid triangle) is from the mutant allele. This mutant allele was designated Int8/5′-dss/t(+2)c, which was a T-to-C transition at the +2 position of the 5′-dss in intron 8. B: One major single peak was detected at the +2 position, representing nucleotide T (indicated by the open triangle) of the normal allele.

The G154V allele resulted in loss of a *Stu*I restriction enzyme recognition site present in exon 5 of the normal LPL allele. The existence of this mutation in patient DI and his parents was examined by detecting a 332-bp band after digestion of the PCR-amplified exon 5 with *Stu*I enzyme. Patient DI and his mother were heterozygous for the G154V allele, while his father was not a carrier (Table 1). Detection of the Int8/5′-dss/t(+2)c allele was performed by mutagenic PCR (artificial introduction of restriction site) as described under Materials and Methods. The existence of the Int8/5′-dss/t(+2)c allele was examined by detecting 31-bp and 243-pb bands after digestion of the mutagenic PCR products of the LPL gene-exon 8 and its boundaries with *Mfe*I enzyme. Patient DI and his father were heterozygous for the Int8/5′-dss/t(+2)c allele, whereas his mother was not a carrier (Table 1).

Effect of the first nucleotide mutation of exon 5 in 3′ splice site on LPL pre-mRNA splicing

The nucleotide G716 (G<u>G</u>^{716}C codon coding Gly^{154}) resides at the first position (+1 position) of exon 5 in the normal LPL gene, which is known to be a consensus sequence [5′-(t/c)$_{10}$ncag/<u>G</u>-3′; the conserved 15 nucleotides and the first nucleotide G of exon is shown by the underline] in 3′-ass. The mutation of a G→T transversion in 3′-ass reduced a score (homology percentage to the conserved sequence of 3′-ass): the score (87.7%) of 3′-ass in the LPL gene without mutation declined to the score (81.4%) with the G-to-T substitution (**Table 2**). Therefore, the G→T transversion in 3′-ass (G<u>G</u>^{716}C→G<u>T</u>^{716}C) might result in aberrant splicing. This possibility was examined by analyzing the size of LPL mRNA transcribed in monocyte-derived macrophage cells from the patient's father, who was a carrier of this mutation (G154V), and a normal subject. The LPL mRNA was reverse-transcribed into LPL cDNA, and the region of LPL cDNA spanning exons 3 and 6 was amplified by the PCR method (**Fig. 3A**). Its size and intensity were determined by agarose electrophoresis. The patient's mother revealed only one band of normal-sized LPL cDNA (424-bp fragment), and its intensity (Fig. 3B, lane 1) was almost the same as that of the control (Fig. 3B, lane 2). Sequencing of the normal-sized LPL cDNA band showed that exon 4 normally joined to exon 5 through a normal skipping of intron 4 (data not shown). These results indicated that the G→T transversion at the first position of exon 5 in 3′-ass of the LPL gene (G<u>G</u>^{716}C→G<u>T</u>^{716}C) was not associated with aberrant splicing.

TABLE 2. Comparison of the consensus regions of 3′ splice site in the LPL, HEXA, and FECH gene with and without the first base mutations in exon

Gene	Allele	15 Nucleotides Constituting 3′ Splice Site	Position (Intron/Exon)	Change of First Base in Exon	Score	Phenotype of Splicing
					%	
LPL	Normal	ttttccctttt*a<u>ag</u>/G	4/5		87.7	
	Mutant	ttttccctttt*a<u>ag</u>/* T	4/5	G→T	81.4	Normal
HEXA	Normal	ccctttcctcc<u>ag</u>/G	12/13		86.4	
	Mutant	ccctttcctcc<u>ag</u>/* A	12/13	G→A	80.6	Normal
FECH	Normal	atcttttcgcat<u>ag</u>/G	8/9		86.0	
	Mutant	atcttttcgcat<u>ag</u>/* T	8/9	G→T	79.8	Exon 9 skipping

The scores were calculated as defined by Shapiro and Senapathy (15) and represent the degree of homology to the highest conserved sequences of 3′ acceptor splice site in primates. The asterisk exhibits mismatched points in comparison with the sequence (5′-(t/c)$_{10}$ncag/G-3′) of the conserved 3′-ass.

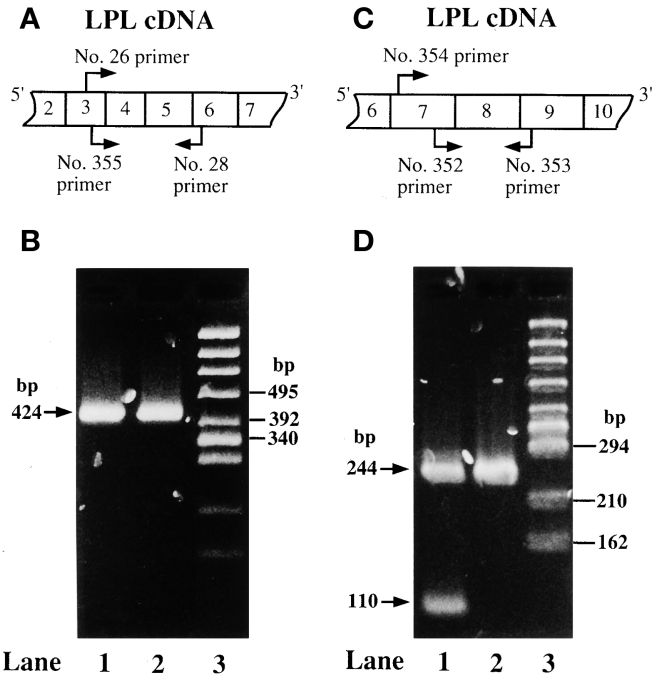

Fig. 3. Schematic illustration of the LPL cDNA amplification after RT reaction of LPL mRNA (A and C) and size determination of the RT-PCR products (B and D). A: Amplification of LPL cDNA (spanning exons 3 through 6) of a normal subject and the patient's mother, who is heterozygous for the G154V allele, was performed by a first PCR using No. 26 primer, followed by a second PCR using a nested primer pair of No. 355 and No. 28. B: The PCR products were separated by 4% NuSieve agarose gel electrophoresis. Lane 1, patient's mother; lane 2, normal subject; lane 3, ΦX 174 DNA size-marker digested with *Hinc*II. C: Amplification of LPL cDNA (spanning exons 7 through 9) of a normal subject and the patient's father, who is heterozygous for the Int8/5′-dss/t(+2)c allele, was performed by first and second PCR using the indicated primers as in A. D: The PCR products were separated by 4% NuSieve agarose gel electrophoresis. Lane 1, patient's father; lane 2, normal subject; lane 3, ΦX 174 DNA size-marker digested with *Hinc*II.

Functional assay of mutant G154V LPL expressed in COS-1 cells

A G^{716}-to-T transversion in 3′-ass of LPL gene exon 5 of the patient's mother presented a possibility of the production of mutant G154V LPL instead of aberrant splicing. The functional significance of the mutant G154V LPL was examined by analyzing the LPL activity and immunoreactive LPL mass expressed in COS-1 cells transfected with the mutant G154V LPL cDNA in comparison with those expressed in COS-1 cells transfected with normal LPL cDNA. The results are summarized in **Table 3**. Mutant G154V LPL activity was not detectable in medium containing LPL released by heparin from the cell surface, or in the cells. No immunoreactive mass of the mutant G154V LPL was released in the medium by heparin treatment, and all the remaining LPL protein was detected in the cells. In contrast, about 51% of the catalytically active normal LPL protein, with a specific activity (the ratio of activity/protein) of 50 ± 1 U/μg, was heparin-releasable, whereas the remaining LPL protein, having a specific activity of 31 ± 2 U/μg, was detected in the cells. Interestingly, the specific activity of the normal LPL released by heparin was about 1.6 times higher than that of the LPL remaining in the cells, suggesting that the LPL released by heparin is a mature form, whereas the intracellular LPL proteins include some precursor LPL molecules which are catalytically inactive. These results suggest that the mutant G154V LPL protein is not adequately transported to the cell surface due to its abnormal structure and, thus, does not become heparin releasable.

The mutant G154V LPL protein that was synthesized in the COS-1 cells was about 28% of the control LPL protein (Table 3). To identify possible factors resulting in the low concentration of G154V LPL, Northern blot analysis was performed. Unexpectedly, the amount of G154V LPL mRNA was almost equal to that of the normal LPL mRNA (data not shown).

Aberrant splicing of LPL pre-mRNA by the Int8/5′-dss/t(+2)c mutation, and structure of abnormally spliced LPL mRNA

The Int8/5′-dss/t(+2)c mutation results from a T-to-C transition at the +2 position in the invariant consensus sequence GT at 5′-dss of intron 8 in the LPL gene, suggesting that this mutation causes aberrant splicing of LPL pre-mRNA. Abnormality of the splicing was examined by

TABLE 3. LPL activity and immunoreactive LPL mass expressed in COS-1 cells transfected with normal LPL cDNA and mutant G154V LPL cDNA

cDNA	Medium Containing LPL Released by Heparin			LPL in Cell Lysate after Heparin Treatment			Total LPL Activity	Total LPL Mass
	Activity	Mass	S.A.[a]	Activity	Mass	S.A.[a]		
	Unit	*ng*	*U/μg*	*Unit*	*ng*	*U/μg*	*Unit*	*ng*
Normal LPL cDNA	8.6 ± 1.4	171 ± 26	50 ± 1	5.2 ± 1.1	167 ± 37	31 ± 2	14 ± 2	338 ± 56
Mutant G154V LPL cDNA	ND	ND		ND	94 ± 17		ND	94 ± 17

The enzyme activity and immunoreactive mass in the medium (1.5 ml) and the cell lysate (2.0 ml) recovered from one dish were quantified by SIIA and sandwich-EIA, respectively. The unit of activity is defined as μmoles/h/1.5 ml for the medium and μmoles/h/2.0 ml for the cell lysate, and the mass value is defined as ng/1.5 ml for the medium and ng/2.0 ml for the cell lysate. The LPL activity and mass values were corrected for differences in transfection efficiency determined by the β-galactosidase activity co-expressed in COS-1 cells. Total LPL activity is the sum of the activities in the medium and the cell lysate, and total LPL mass is the sum of the masses in the medium and the cell lysate. Each experiment was performed using four distinct dishes, and both the activity and mass values are shown as the mean ± SD. ND, not detectable.

[a] S.A., specific activity; calculated by dividing the LPL activity by the LPL mass.

analyzing the size of LPL mRNA transcribed in monocyte-derived macrophage cells of patient's father, who was heterozygous for the Int8/5′-dss/t(+2)c mutation. The LPL mRNA was reverse transcribed into LPL cDNA, and the region of LPL cDNA spanning exons 7 and 9 was amplified by the PCR method (Fig. 3C). Its size and intensity were determined by agarose electrophoresis. As shown in Fig. 3D, the patient's father revealed two bands: a normal-sized LPL cDNA band (244-bp fragment) and a 110-bp fragment band shorter than the normal one (lane 1). The normal subject showed only one LPL cDNA band (244-bp fragment; lane 2). As expected, the intensity of the normal-sized LPL cDNA in the patient's father (lane 1) was about half that of the normal subject (lane 2), suggesting that this is from only the normal LPL allele and that the Int8/5′-dss/t(+2)c allele produces shorter aberrant LPL cDNA by a complete abnormal splicing (Fig. 3D).

The structure of abnormally spliced LPL cDNA (110-bp fragment) and normal-sized LPL cDNA (244-bp fragment) was examined by sequencing both DNA fragments. Sequencing of the abnormally spliced one revealed that a part of exon 8 was joined to exon 9 because of skipping 134 bases of exon 8 (nucleotides 1363 through 1496) and intron 8 (**Fig. 4A** and **B**). This aberrant junction resulted in a frame shift with a stop codon (TAG), which was six codons downstream from the codon for Glu^{369} (Fig. 4A). Sequencing of the normal-sized LPL cDNA revealed that exon 8 normally joined to exon 9 through a normal skipping of intron 8 in which the last AA dinucleotides in exon 8 and the first G nucleotide in exon 9 encode AA/G for Lys^{414} (Fig. 4B and 4C). These results indicated that a T-to-C transition in the invariant GT of 5′-dss in intron 8 completely inactivated the authentic 5′ splice site, and a G(−133)T dinucleotide in exon 8 was alternatively used as a cryptic 5′-dss (No. 2; 5′-GAG/GTAGAT-3′; **Table 4**).

DISCUSSION

In the present study, we described in detail the biochemical and genetic characterizations of two novel mutations in the LPL gene of a Japanese male infant (patient DI) with severe fasting hyperchylomicronemia due to primary LPL deficiency. Patient DI showed no LPL activity in PHP and almost no immunoreactive LPL mass in PHP due to compound heterozygosity for a G-to-T transversion mutation (G/GC→G/TC) in the first nucleotide at position 716 of exon 5 (+1 position of 3′-ass in intron 4) and a T-to-C transition mutation in the invariant GT at the second (+2) position of 5′-dss in intron 8 (Int8/5′-dss/t(+2)c).

Notably, the G-to-T transversion at 3′-ass of intron 4 (5′-$(t/c)_{10}$taag/T-3′) described here occurs at the first nucleotide of exon 5 of the LPL gene, which is within the 3′-consensus acceptor sequence for splicing (5′-$(t/c)_{10}$ncag/G-3′; G is the first base in exon) (15, 16). This is a good model for elucidating the relationship between mutation

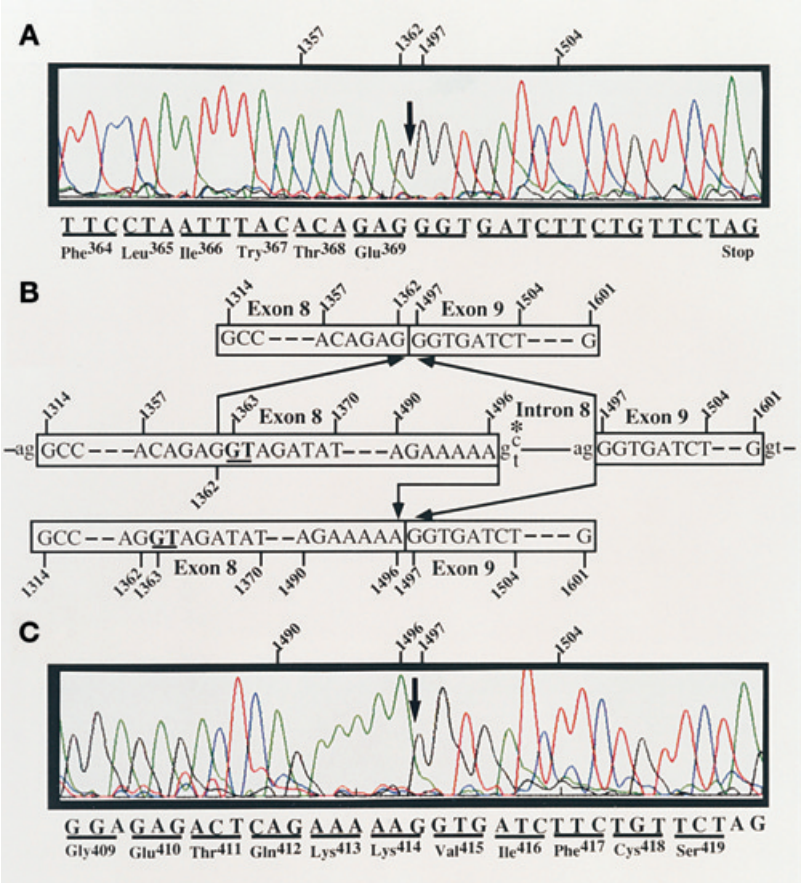

Fig. 4. Sequencing of the aberrant 110-bp and the normal-sized 244-bp cDNA fragments of RT-PCR products of LPL mRNA. The 110-bp and 244-bp cDNA fragments of the patient's father, separated by 4% NuSieve gel in lane 1 of Fig. 3D, were extracted, cloned into a pCRII vector, and sequenced. A and C: Nucleotide sequence patterns of a part of the sense strand of the aberrant 110-bp fragment (A) and the normal-sized 244-bp fragment (C) are shown. The joints of exon 8 and exon 9 are shown by the solid arrows, respectively. B: Aberrant splicing due to a T-to-C (indicated by the asterisk) transition in the invariant GT of the 5′ donor splice site in intron 8 of the LPL gene and normal splicing in the allele without the mutation are schematically illustrated. In the aberrant splicing, a GT dinucleotide (indicated by the bold letters and the underline; guanosine's position is 1363) in exon 8 was used as a cryptic 5′ donor splice site, resulting in the connection of the 3′ end of the G^{1362} in exon 8 to the G^{1497} of the first nucleotide in exon 9. In contrast, the sequence pattern of the normal-sized cDNA fragment revealed a normally spliced LPL transcript skipping intron 8, resulting in the connection of the A^{1496} of the last base in exon 8 to the G^{1497} of the first base in exon 9.

TABLE 4. Comparison of potential cryptic splice sites with the authentic 5′ donor splice site in intron 8 of the LPL gene

No.	Nine Nucleotides Constituting 5′ Splice Site	Position[a]	Score	Delta G
			%	*kcal/mol*
1	GAAGTTTCC	−176	45	1.3
2	GAGGTAGAT	−133	73	−4.9
3	CATGTTGAA	−111	49	0.3
4	AGAGTGATT	−91	63	0.1
5	CTGGTCAGA	−72	77	−2.5
6	CTGGTGGAG	−63	61	−2.8
7	GCAGTCCCG	−55	39	1.3
8	AGAGTAAAA	−26	61	−0.7
9	AAAGTAATT	+1	73	−0.7
10	AATGTATTT	+11	62	0.2
11	GATGTCAGG	+47	71	0.4
12	GCTGTATTT	+64	52	0.2
13	CTTGTATTT	+110	46	0.2
14	ACTGTATGA	+122	53	0.2
15	GATGTAGAT	+129	51	−0.3
16	GGAGTCTTC	+146	38	1.3
17	GAAGTGACA	+187	63	0.1
18	ACAGTATTT	+193	45	0.2
19	TTTGTATTT	+201	51	0.2

The scores were calculated according to the method of Shapiro and Senapathy (15) and represent the degree of homology to the highest conserved 5′ splice site in primates. The Delta G values were calculated using the parameters proposed by Freier et al. (32) and represent the free-energy change for binding to U1 snRNA.

[a] The minus and plus numbers indicate the G positions of the respective underlined GT dinucleotides in exon 8 (No. 1–8) (6,7) and intron 8 (No. 9–19) (28). The authentic 5′-dss at the +1 position in intron 8 is shown in No. 9.

of the first nucleotide in exon at 3′-ass in the LPL gene and LPL pre-mRNA splicing. In primates, G is the most common base at the first position (+1) of 3′-ass, observed at a frequency of 49%, while A, C, and T are seen at frequencies of 28%, 13%, and 10%, respectively (15). In the LPL gene, guanosine is indeed the most common base at the first position of 3′-ass, observed at a frequency of 56%, while exons 2, 6, and 10 begin with A (33%), and exon 7 with T (11%). Therefore, we examined whether or not the G-to-T substitution at the first nucleotide of exon 5 in the LPL gene, in which the G utilized at the highest frequency is replaced by the T used at the lowest frequency, causes aberrant splicing. RT-PCR analysis of LPL mRNA, isolated from monocyte-derived macrophages of the patient's mother who is a carrier of the G-to-T transversion mutation in exon 5, revealed only a normal-sized cDNA band spanning exons 3 through 6, with the same intensity as the control (Fig. 3B). Sequencing of the normal-sized cDNA subcloned into a pCRII vector showed the normal junction between exons 4 and 5. These findings indicate that the G-to-T transversion mutation at the first nucleotide of exon 5 in the LPL gene is a leaky recognition for splicing, resulting in a missense mutation of G154V ($GG^{716}C \rightarrow GT^{716}C$/$Gly^{154} \rightarrow Val$). Furthermore, when the sequence of $(t/c)_{10}$nnag/N, which may play a role as a potential cryptic site in place of the variant authentic 3′-ass $[(t/c)_{10}taag/T]$ of our patient's LPL gene, was searched against the DNA sequences (214 bp through 1,200 bp) of the human LPL gene (28) including a part of exon 4, intron 4, exon 5, and a part of intron 5, it was only found at the place of the variant authentic 3′-ass. This may be also a reason why no alternative splicing was detected in this mutation.

Similarly, the involvement of the first nucleotide's mutation in exon at the 3′-ass to splicing has been reported in a few other genes such as ferrochelatase (FECH) (20), beta-hexosaminidase A (HEXA) (21), and RH antigens (RHAG) (22). In fact, a G-to-C transversion at the first base of exon 13 in the HEXA gene and a G-to-A transition at the first base of exon 6 in the RHAG gene produced only normally spliced mRNA, and resulted in a missense mutation. On the other hand, a G-to-T transversion at the first base of exon 9 in the FECH gene caused complete aberrant splicing with skipping of exon 9, whereas a G-to-T transversion at the first base of exon 9 in the RHAG gene caused partial aberrant splicing: mainly normally spliced mRNA and a minor fraction with skipping of exon 9. These reports indicate that changes of the first G nucleotide in exons at the 3′-ass to other nucleotides (A, C, or T) lead to normal splicing or aberrant splicing. To gain some factors for splice site selection, we compared the sequences of 15 nucleotides constituting 3′-ass in LPL, HEXA, and FECH genes in which the sequences of 3′ splice junction sites were available (Table 2). Among three genes, the substitution of the first G base of exons to T or A reduced, almost equally, the percentage of the score (the degree of homology to the highest conserved 3′-ass), but the 3′-ass sites for LPL and HEXA were normally utilized and the 3′-ass for FECH was inactivated due to the substitution of the first G of exon to T. Interestingly, all 10 pyrimidines within the pyrimidine tract are conserved in the 3′-ass of LPL and HEXA genes, whereas the 3′-ass of FECH gene revealed two substitutions of pyrimidine to purine at −6 and −14 positions from the invariant "g" in intron 8 (Table 2). This may imply that an additional substitution of the first G

base in exon to other bases (in the 3′-ass with the changes of pyrimidine to purine within pyrimidine tract) is susceptible to the functional defect of 3′-ass.

The functional significance of the G154V LPL was confirmed to be catalytically inactive and nonheparin releasable from the cells by an in vitro expression study in COS-1 cells. The catalytic defect in the mutant G154V LPL might be explained by elucidation of the superimpositional structure between the three-dimensional crystallographic structure of human pancreatic lipase and human LPL (29–31). This Gly→Val mutation occurs in the central beta-strand structure of the Arg-Ile-Thr-Gly154-Leu-Asp156 motif in the N-terminal domain (residues 1–312, derived from exons 1 through 6) containing the catalytic triad residues (Ser132-Asp156-His241) (30). The substitution of Gly154 to Val causes conversion of a neutral small amino acid to a hydrophobic amino acid with a larger side chain. Therefore, this substitution may change the conformation of the beta-sheet structure and, subsequently, disrupt the spatial configuration of this critical region for the catalytic triad. As a result, the mutant G154V LPL becomes a catalytically inactive enzyme.

Molecular characterization of the mutant Int8/5′-dss/t(+2)c LPL allele, one of the compound heterozygous LPL mutations carried by patient DI, was determined by RT-PCR analysis of LPL mRNA isolated from monocyte-derived macrophages of the patient's father, who was a carrier of the Int8/5′-dss/t(+2)c LPL allele. The transition (GT→GC) in the invariant GT of 5′-dss in intron 8 of the LPL gene completely inactivated the authentic 5′ splice site and led to the utilization of a cryptic splice site in exon 8. To gain insight into the mechanism of splice site selection in vivo, we compared the characteristics of the 18 potential cryptic splice sites (GT-containing nine nucleotides in exon 8 and intron 8) with that of the authentic 5′-dss (Table 3). Only three (Nos. 2, 5, and 11) of the 18 potential cryptic splice sites revealed scores above 70%, representing the degree of homology to the highest conserved 5′-dss in primates (15), and also favorable free-energy values for interaction between the cryptic splice site and U1 snRNA (32). As expected, one (No. 2; GAGGTAGAT at position −133 in exon 8) of the three candidates was indeed utilized as the cryptic splice site in exon 8, and its score was as high as that (73%) of the authentic 5′-dss (No. 9; AAAGTAATT at position +1 of intron 8). On the other hand, one (No. 5; CTGGTCAGA at position −72 in exon 8) of the three candidates showed the highest score of 77%, and a favorable free energy of −2.5 kcal/mol, but it was not utilized as a cryptic splice site in exon 8. Therefore, in addition to these two parameters, other undetermined factors may be involved in properly selecting the 5′-dss in vivo. The adequate distance from the authentic splice site and/or the overall RNA structure surrounding the cryptic splice site might be another important determinant for the selection of the cryptic splice sites.

The activated cryptic splice site in exon 8, due to the G-to-C transversion (Int8/5′-dss/t(+2)c) in the invariant GT of intron 8 of the LPL gene, resulted in aberrant splicing: a part of exon 8 lacking a 134-bp fragment (nucleotides 1363–1496 in exon 8) was joined to exon 9. This aberrant joint inevitably resulted in a frameshift that generated a stop codon. This predicts production of the truncated LPL molecule lacking amino acid sequences of Val^{370}–Gly^{448} (e.g., Val^{370}–Lys^{414} and Arg^{420}–Gly^{448}), which are a part of the carboxyl C-terminal domain (residues 313–448 in exons 7 to 9) containing the substrate-binding (33) and heparin-binding regions (34). Essentially, the truncated LPL molecule is presumed to be catalytically inactive due to a lack of the essential region for interaction with substrates such as chylomicrons and VLDL.

In this study, we reported in detail the effect of a T-to-C transition in the invariant GT at 5′-dss of intron 8 and a substitution of the first G base to T base in exon 5 at 3′-ass of intron 4 on LPL pre-mRNA splicing. The T-to-C substitution in the invariant GT of intron 8 inactivated completely the authentic 5′-dss, and led to the utilization of a cryptic splice site in exon 8 among three putative candidates with relatively higher parameters (homology to the highest conserved sequences of the 5′-dss and free energy to the U1 snRNA binding) than other candidates. Selection of the cryptic splice site, however, could not be explained only by the two parameters. The overall RNA structure surrounding the candidate sequences may be one of the important factors for splice site selection in vivo. Our additional mutation of the first G base to T in exon 5 at the 3′-ass of intron 4 in the LPL gene may help us to better understand important factors that involve the selection of 3′-ass in vivo.

We thank Dr. Tokio Tani, Kyusyu University, for assistance of the free-energy calculation for RNA duplex formation. This research was supported, in part, by Grants-in-Aid for Scientific Research (C) (No. 11670402 and No. 12670384) from the Ministry of Education, Science, and Culture of Japan.

Manuscript received 29 September 2000, in revised form 28 November 2000, in re-revised form 29 January 2001, and in re-re-revised form 12 March 2001.

REFERENCES

1. Havel, R. J., J. L. Goldstein, and M. S. Brown. 1980. Lipoproteins and lipid transport. *In* Metabolic Control and Disease. P. K. Bondy and L. E. Rosenberg, editors. Saunders, Philadelphia, PA. 393–494.
2. Brunzell, J. D. 1995. Familial lipoprotein lipase deficiency and other causes of the chylomicronemia syndrome. *In* The Metabolic and Molecular Bases of Inherited Disease. C. R. Scriver, A. L. Beaudet, W. S. Sly, and D. Valle, editors. McGraw-Hill, New York. 1913–1932.
3. Ikeda, Y., A. Takagi, and A. Yamamoto. 1989. Purification and characterization of lipoprotein lipase and hepatic triglyceride lipase from human postheparin plasma: production of monospecific antibody to the individual lipase. *Biochim. Biophys. Acta.* **1003:** 254–269.
4. Wion, K. L., T. G. Kirchgessner, A. J. Lusis, M. C. Schotz, and R. M. Lawn. 1987. Human lipoprotein lipase complementary DNA sequence. *Science.* **235:** 1638–1641.
5. Sparkes, R. S., S. Zollman, I. Klisak, T. G. Kirchgessner, M. C. Komaromy, T. Mohandas, M. C. Schotz, and A. J. Lusis. 1987. Human genes involved in lipolysis of plasma lipoproteins: mapping of loci for lipoprotein lipase to 8p22 and hepatic lipase to 15q21. *Genomics.* **1:** 138–144.
6. Deeb, S. S., and R. Peng. 1989. Structure of the human lipoprotein lipase gene. *Biochemistry.* **28:** 4131–4135.
7. Kirchgessner, T. G., J-C. Chuat, C. Heinzmann, J. Etienne, S.

Guilhot, K. Svenson, D. Ameis, C. Pilon, L. d'Auriol, A. Andalibi, M. C. Schotz, F. Galibert, and A. J. Lusis. 1989. Organization of the human lipoprotein lipase gene and evolution of the lipase gene family. *Proc. Natl. Acad. Sci. USA*. **86:** 9647–9651.
8. Oka, K., G. T. Tkalcevic, T. Nakano, H. Tucker, K. Ishimura-Oka, and W. V. Brown. 1990. Structure and polymorphic map of human lipoprotein lipase gene. *Biochim. Biophys. Acta.* **1049:** 21–26.
9. Olivecrona, T., G. Bengtsson, S. E. Marklund, U. Lindahl, and M. Hook. 1977. Heparin-lipoprotein lipase interactions. *Fed. Proc.* **36:** 60–65.
10. Misra, K. B., K. C. Kim, S. Cho, M. G. Low, and A. Bensadoun. 1994. Purification and characterization of adipocyte heparan sulfate proteoglycans with affinity for lipoprotein lipase. *J. Biol. Chem.* **269:** 23838–23844.
11. Krauss, R. M., R. I. Levy, and D. S. Fredrickson. 1974. Selective measurement of two lipase activities in postheparin plasma from normal subjects and patients with hyperlipoproteinemia. *J. Clin. Invest.* **54:** 1107–1124.
12. Ikeda, Y., A. Takagi, Y. Ohkaru, K. Nogi, T. Iwanaga, S. Kurooka, and A. Yamamoto. 1990. A sandwich-enzyme immunoassay for the quantification of lipoprotein lipase and hepatic triglyceride lipase in human postheparin plasma using monoclonal antibodies to the corresponding enzymes. *J. Lipid Res.* **31:** 1911–1924.
13. Jackson, R. L. 1983. Lipoprotein lipase and hepatic lipase. *In* The Enzymes. Vol. 16. P. D. Boyer, editor. Academic Press, New York. 141–181.
14. Santamarina-Fojo, S., and K. A. Dugi. 1994. Structure, function and role of lipoprotein lipase in lipoprotein metabolism. *Curr. Opin. Lipidol.* **5:** 117–125.
15. Shapiro, M. B., and P. Senapathy. 1987. RNA splice junctions of different classes of eukaryotes: sequence statistics and functional implications in gene expression. *Nucleic Acids Res.* **15:** 7155–7174.
16. Krawczak, M., J. Reiss, and D. N. Cooper. 1992. The mutational spectrum of single base-pair substitutions in mRNA splice junctions of human genes: causes and consequences. *Hum. Genet.* **90:** 41–54.
17. Hata, A., M. Emi, G. Luc, A. Basdevant, P. Gambert, P. H. Iverius, and J. M. Lalouel. 1990. Compound heterozygote for lipoprotein lipase deficiency: Ser→Thr244 and transition in 3′ splice site of intron 2 (AG→AA) in the lipoprotein lipase gene. *Am. J. Hum. Genet.* **47:** 721–726.
18. Gotoda, T., N. Yamada, M. Kawamura, K. Kozaki, N. Mori, S. Ishibashi, H. Shimano, F. Takaku, Y. Yazaki, Y. Furuichi, and T. Murase. 1991. Heterogeneous mutations in the human lipoprotein lipase gene in patients with familial lipoprotein lipase deficiency. *J. Clin. Invest.* **88:** 1856–1864.
19. Chimienti, G., A. Capurso, F. Resta, and G. Pepe. 1992. A G→C change at the donor splice site of intron 1 causes lipoprotein lipase deficiency in a southern-Italian family. *Biochem. Biophys. Res. Commun.* **187:** 620–627.
20. Wang, X., M. Poh-Fitzpatrick, T. Chen, K. Malavade, D. Carriero, and S. Piomelli. 1995. Systematic screening for RNA with skipped exons—splicing mutations of the ferrochelatase gene. *Biochim. Biophys. Acta.* **1271:** 358–362.
21. Petroulakis, E., Z. Cao, J. T. Clarke, D. J. Mahuran, G. Lee, and B. Triggs-Raine. 1998. W474C amino acid substitution affects early processing of the alpha-subunit of beta-hexosaminidase A and is associated with subacute G(M2) gangliosidosis. *Hum. Mutat.* **11:** 432–442.
22. Huang, C. H., G. Cheng, Z. Liu, Y. Chen, M. E. Reid, G. Halverson, and Y. Okubo. 1999. Molecular basis for Rh(null) syndrome: identification of three new missense mutations in the Rh 50 glycoprotein gene. *Am. J. Hematol.* **62:** 25–32.
23. Hatch, F. T., and R. S. Lees. 1968. Practical methods for plasma lipoprotein analysis. *Adv. Lipid Res.* **6:** 1–68.
24. Takagi, A., Y. Ikeda, and A. Yamamoto. 1990. DNA sequence of lipoprotein lipase cDNA cloned from human monocytic leukemia THP-1 cells. *Nucleic Acids Res.* **18:** 6436.
25. Maniatis, T., E. F. Fritsch, and J. Sambrook. 1982. Molecular Cloning: A Laboratory Manual. Cold Spring Harbor Laboratory Press, Cold Spring Harbor, NY.
26. Ikeda, Y., K. Goji, and A. Takagi. 2000. A compound heterozygote for a novel missense mutation (G105R) in exon 3 and a missense mutation (D204E) in exon 5 of the lipoprotein lipase gene in a Japanese infant with hyperchylomicronaemia. *Clin. Sci.* **99:** 569–578.
27. Takagi, A., Y. Ikeda, Z. Tsutsumi, T. Shoji, and A. Yamamoto. 1992. Molecular studies on primary lipoprotein lipase (LPL) deficiency: one base deletion (G^{916}) in exon 5 of LPL gene causes no detectable LPL protein due to the absence of LPL messenger RNA transcript. *J. Clin. Invest.* **89:** 581–591.
28. Nickerson, D. A., S. L. Taylor, K. M. Weiss, A. G. Clark, R. G. Hutchinson, J. Stengard, V. Salomaa, E. Vartiainen, E. Boerwinkle, and C. F. Sing. 1998. DNA sequence diversity in a 9.7-kb region of the human lipoprotein lipase gene. *Nat. Genet.* **19:** 233–240.
29. Winkler, F. K., A. D'Arcy, and W. Hunziker. 1990. Structure of human pancreatic lipase. *Nature.* **343:** 771–774.
30. Derewenda, Z. S., and C. Cambillau. 1991. Effects of gene mutations in lipoprotein and hepatic lipases as interpreted by a molecular model of the pancreatic triglyceride lipase. *J. Biol. Chem.* **266:** 23112–23119.
31. van Tilbeurgh, H., A. Roussel, J. M. Lalouel, and C. Cambillau. 1994. Lipoprotein lipase. Molecular model based on the pancreatic lipase x-ray structure: consequences for heparin binding and catalysis. *J. Biol. Chem.* **269:** 4626–4633.
32. Freier, S. M., R. Kierzek, J. A. Jaeger, N. Sugimoto, M. H. Caruthers, T. Neilson, and D. H. Turner. 1986. Improved free-energy parameters for predictions of RNA duplex stability. *Proc. Natl. Acad. Sci. USA.* **83:** 9373–9377.
33. Lookene, A., and G. Bengtsson-Olivecrona. 1993. Chymotryptic cleavage of lipoprotein lipase. Identification of cleavage sites and functional studies of the truncated molecule. *Eur. J. Biochem.* **213:** 185–194.
34. Sendak, R. A., and A. Bensadoun. 1998. Identification of a heparin-binding domain in the distal carboxyl-terminal region of lipoprotein lipase by site-directed mutagenesis. *J. Lipid Res.* **39:** 1310–1315.